Treatment of Organic Compounds by Activated Persulfate Using Nanoscale Zerovalent Iron

ARTICLE *in* INDUSTRIAL & ENGINEERING CHEMISTRY RESEARCH · SEPTEMBER 2013

Impact Factor: 2.59 · DOI: 10.1021/ie400387p

I&EC research
Industrial & Engineering Chemistry Research

Article

pubs.acs.org/IECR

Treatment of Organic Compounds by Activated Persulfate Using Nanoscale Zerovalent Iron

Mohammed A. Al-Shamsi and Neil R. Thomson*

Department of Civil & Environmental Engineering, University of Waterloo, 200 University Avenue West, Waterloo, Ontario, Canada N2L 3G1

Supporting Information

ABSTRACT: Recently, persulfate has caught the attention of groundwater remediation practitioners as a promising oxidant for in situ chemical oxidation. In this study, a method was applied to treat a selection of hazardous organic compounds using nanoscale zerovalent iron (nZVI) particles as activators for persulfate. The results show that degradation of these organic compounds using nZVI-activated persulfate is more effective than nZVI alone. For example, the degradation of naphthalene by nZVI-activated persulfate was >99% compared to <10% by nZVI alone. Despite the higher effectiveness, the nZVI particles were passivated quickly following exposure to persulfate, causing the reaction rate to reduce to a magnitude representative of an unactivated persulfate system. X-ray photoelectron spectroscopy analyses indicated that an iron sulfate layer was formed on the nZVI particle surfaces following exposure to persulfate compared to the FeOOH layer that was present on the fresh nZVI surfaces. Although the nZVI particle surfaces are passivated, nZVI appears to be a promising persulfate activator compared to the conventional persulfate activators such as Fe^{2+} and granular ZVI.

1. INTRODUCTION

Many of the organic compounds used widely by industry are classified as hazardous and toxic substances and thus threaten human and ecosystem health. Some of these organic compounds are known potential human carcinogens such as trichloroethylene (TCE; an industrial solvent),[1,2] methyl *tert*-butyl ether (MTBE; a gasoline additive),[3] naphthalene (a petroleum and coal tar product),[4] and chlorobenzene (used widely in the pesticide manufacturing process).[5] Effective treatment solutions for soil and groundwater contaminated with hazardous organic compounds are required by remediation scientists and engineers.

In situ chemical oxidation is a promising technology that can be used to oxidize a wide range of organic compounds.[6] Hydrogen peroxide,[7] permanganate,[8] and ozone[9] have been used in the subsurface, and recently persulfate[10,11] has gained popularity because of its stability in the subsurface and high oxidation potential (E_h = 2.01 V):

$$S_2O_8^{2-} + 2e^- \rightarrow 2SO_4^{2-} \quad (1)$$

The treatment of some organic compounds can be enhanced and accelerated by employing activation methods. Activation methods can generate the sulfate free radical ($SO_4^{\bullet-}$) from persulfate, which is a much stronger oxidant (E_h = 2.6 V) than the persulfate anion. When transition metals are used (denoted by M^{n+}), then the following reaction can occur:[12]

$$M^{n+} + S_2O_8^{2-} \rightarrow M^{n+1} + SO_4^{2-} + SO_4^{\bullet-} \quad (2)$$

Sulfate free radicals can produce hydroxyl free radicals ($OH^{\bullet}$), which are less selective than sulfate free radicals with a higher redox potential [$E_h(OH^{\bullet}/OH^-)$ = 2.7 V]:[12,13]

$$SO_4^{\bullet-} + H_2O \rightarrow SO_4^{2-} + OH^{\bullet} + H^+ \qquad K[H_2O] = 2 \times 10^{-3}\ s^{-1} \quad (3)$$

$$SO_4^{\bullet-} + OH^- \rightarrow SO_4^{2-} + OH^{\bullet} \qquad K = 6.5 \times 10^7\ M^{-1}\ s^{-1} \quad (4)$$

These free radicals can attack organic compounds and break them down to nontoxic or less toxic compounds.[14,15]

Iron was used initially in a soluble form (dissolved phase) as the ferrous ion (Fe^{2+}) to activate persulfate;[16] however, aqueous Fe^{2+} is relatively insoluble at the ambient pH ≥ 5 of most aquifer systems.[17] A variety of chelating agents (e.g., ethylenediaminetetraacetic acid, diethylenetriamine pentaacetic acid, and nitrilotriacetic acid) are normally used to enhance the solubility of iron. Chelating agents are organic-based compounds that can be degraded in the presence of an oxidant, and they also compete with the target organic compounds for the oxidant and the generated free radicals in the system.[17,18]

As an alternative activator, zerovalent iron (ZVI), an insoluble form of iron, has been employed with promising results.[19−22] However, because of the small pore size associated with geological porous media, ZVI in a granular form (millimeter) or powder form (micrometer) cannot be injected into the subsurface and, hence, is not suitable.

In this study, we use nanoscale ZVI (nZVI) to activate persulfate and to treat an aqueous organic compound of interest. Our objective was to investigate the treatment of

Received: February 1, 2013
Revised: July 30, 2013
Accepted: August 3, 2013
Published: August 21, 2013

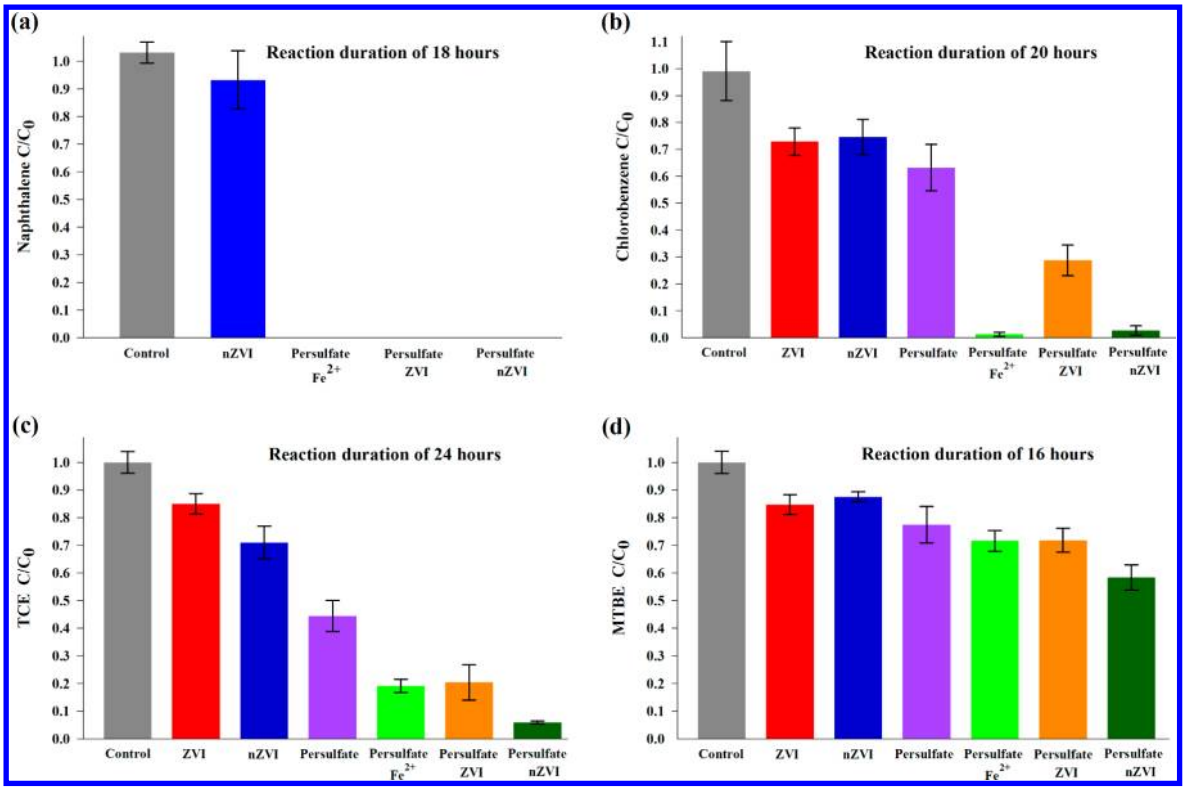

Figure 1. Degradation of (a) naphthalene, (b) chlorobenzene, (c) TCE, and (d) MTBE for the various treatment systems investigated. The error bars represent the standard deviation from five replicates. Naphthalene data were <MDL for the three activated persulfate systems (persulfate/Fe^{2+}, persulfate/ZVI, and persulfate/nZVI). Naphthalene data for the granular-ZVI-only system (ZVI) and the unactivated persulfate system (persulfate) are not available.

selected organic compounds (e.g., TCE, MTBE, naphthalene, and chlorobenzene) by persulfate in the presence of a variety of iron activators (i.e., nZVI, granular ZVI, and Fe^{2+}). The findings from this work advance our understanding of the role of nZVI as a persulfate activator.

In terms of reaction mechanisms, ZVI can activate persulfate by three possible mechanisms (all of these mechanisms can generate Fe^{2+} through ZVI corrosion): (1) direct release of Fe^{2+} by persulfate, (2) indirect release of Fe^{2+} by oxygenated water, and (3) indirect release of Fe^{2+} in deoxygenated water as given by[20,23]

$$Fe^0 + S_2O_8^{2-} \rightarrow Fe^{2+} + 2SO_4^{2-} \quad (5)$$

$$Fe^0 + \frac{1}{2}O_2 + H_2O \rightarrow Fe^{2+} + 2OH^- \quad (6)$$

$$Fe^0 + 2H_2O \rightarrow Fe^{2+} + 2OH^- + H_2 \quad (7)$$

Corrosion of the ZVI surface, in the direct reaction pathway, is much faster than corrosion taking place along the other two pathways. Following release from ZVI, Fe^{2+} can activate persulfate to generate sulfate free radicals by[21,22]

$$Fe^{2+} + S_2O_8^{2-} \rightarrow Fe^{3+} + SO_4^{2-} + SO_4^{\bullet-}$$
$$K = 2 \times 10^1\ M^{-1}\ s^{-1} \quad (8)$$

However, at higher ZVI dosages, a chain of inhibiting reactions (radical scavenging reactions) occurs, and this reduces treatment effectiveness. The reaction rates of these radical scavenging reactions are much faster than the free-radical formation reactions as shown by[21,22,24]

$$Fe^{2+} + SO_4^{\bullet-} \rightarrow Fe^{3+} + SO_4^{2-}$$
$$K = 4.6 \times 10^9\ M^{-1}\ s^{-1} \quad (9)$$

Also, Fe^{2+} can be recycled by reaction with Fe^{3+} that is present with the ZVI surface as follows:[22]

$$2Fe^{3+} + Fe^0 \rightarrow 3Fe^{2+} \quad (10)$$

2. MATERIALS AND METHODS

2.1. Materials and Chemicals. The following materials were assembled: nZVI particles (average particle size 66−187 nm with a specific surface area of 37−58 $m^2\ g^{-1}$) from Polymetallix; granular ZVI (1000−2000 μm size, 99.98%) from Alfa Aesar; ferrous sulfate and 7-hydrate granular (99.86%) from J. T. Baker; trichloroethylene (TCE; 99.8%), naphthalene (99%), and chlorobenzene (99.5%) from BDH; sodium persulfate (≥98%), hydroxylamine (99%), 1,10-phenanthroline monohydrate (99%), ammonium acetate (>98%), and sodium bicarbonate (99.5%) from Sigma-Aldrich; potassium iodide (>99%) and hydrochloric acid (34−37%) from EMD Chemicals Inc.; and MTBE (99.95%) from EM Science. All chemicals were of reagent grade and were used as received.

2.2. Procedures and Preparation. The stock solutions of persulfate and the organic compounds were prepared by mixing the desired amount of laboratory-grade chemicals and Milli-Q water (resistivity of 18.2 MΩ cm^{-1}). All of the aqueous experiments were performed in 40 mL batch reactors [borosilicate glass vial fitted with poly(tetrafluoroethylene) septa]. The solutions were added to each reactor starting with the persulfate solution, then the organic solution (TCE, MTBE, napthalene, or chlorobenzene solutions), then the activators

dx.doi.org/10.1021/ie400387p | Ind. Eng. Chem. Res. 2013, 52, 13564−13571

(soluble Fe^{2+}, granular ZVI, or nZVI), and finally the reactors (three to five treatment replicates) were filled with Milli-Q water (zero headspace) and placed on an orbital shaker (200 rpm) in a dark room (temperature 20.5 ± 4 °C). nZVI and ZVI were added as received. At the selected sampling times, a gastight syringe (1 mL; 1001 Hamilton syringe series, Sigma-Aldrich) was used to collect aqueous samples through the reactor septa for organic compound and persulfate analyses.

A range of TCE/persulfate/activator molar ratios from 1:20:0 (for the unactivated persulfate system) to 1:40:150 were explored, and the initial concentration of TCE was 50 or 375 mg L^{-1}. To determine the optimal TCE treatment capability, a sequence of experiments were performed using different nZVI and persulfate molar ratios. For the other organic compounds, a 1:20:20 molar ratio of organic compound/persulfate/activator was used, and the initial concentrations of MTBE, naphthalene, and chlorobenzene were 300, 13, and 300 mg L^{-1}, respectively.

2.3. Analysis. Samples (0.7 mL) for organic compound analyses were injected into 2 mL glass vials and shaken on a mini vortexer (VWR Scientific) for 10 s prior to gas chromatography analysis. The organic compound concentration was determined by a headspace solid-phase microextraction (HS-SPME) method[25] using a HP 6890 series gas chromatograph equipped with a flame ionization detector, with column length 30 m × 0.53 mm and 0.5 μm film (Supelco), a 100 μm SPME fiber coated with poly(dimethylsiloxane) (Supelco), and a Varian 8200 series autosampler.

Persulfate was determined by the spectrophotometric method developed by Liang et al.[26] with slight modifications. Potassium iodide (100 g), sodium bicarbonate (5 g), and 100 mL of Milli-Q water were mixed to create a stock solution. A 4 mL aliquot was taken from the stock solution using a pipet and added to 0.1 mL of a persulfate sample, and then 36 mL of Milli-Q water was added. The concentration of persulfate was measured spectrophotometrically (after 15 min) using a HACH spectrophotometer (DR/2010) at 400 nm.

The total iron, dissolved iron, and ferrous ion were analyzed spectrophotometrically using 1,10-phenanthroline monohydrate as the detector with a HACH spectrophotometer (DR/2010) at 500 nm.[27] Suspended or solid iron was estimated as the difference between the total iron and dissolved iron, and the ferric iron was estimated as the difference between the dissolved iron and ferrous iron. We assumed that the nZVI particles that were added were 100% metallic iron and neglected the thin iron oxide shell.

The surface of the nanoiron particles was characterized by X-ray photoelectron spectroscopy (XPS; Thermo-VG Scientific ESCALab 250). XPS spectra were analyzed by using the *CasaXPS* software (version 2.3.15; CasaXPS Software Ltd.). All spectra were calibrated against a carbon peak (C1 s) at a binding energy (BE) of 284.6 eV.

Aqueous pH and E_h were determined using a pH/ISE meter (Orion 710A) and a pH/ISE meter (Orion 4 star, Thermo Electron Corp.).

3. RESULTS AND DISCUSSION

3.1. Chemical Oxidation versus Chemical Reduction. The naphthalene concentration was below the method detection limit (<MDL) using activated persulfate (for all three activator systems), while the remaining naphthalene concentration was >90% of the initial naphthalene concentration for the nZVI only system (Figure 1a). The data for naphthalene for the unactivated persulfate system and the granular-ZVI-only system are not available.

The remaining chlorobenzene concentration was <3% of the initial chlorobenzene concentration using the Fe^{2+}- and nZVI-activated persulfate system and 29% using the granular-ZVI-activated persulfate system, while the chlorobenzene concentration was >70% of the initial chlorobenzene concentration using either granular ZVI or nZVI (Figure 1b).

In the case of TCE, the remaining TCE concentration was <6% of the initial TCE concentration using the nZVI-activated persulfate system compared to 70% using the nZVI only system. Similarly, the remaining TCE concentration was ∼20% of the initial TCE concentration using granular-ZVI-activated persulfate compared to >85% using the granular-ZVI-only system (Figure 1c). The results from a statistical analysis showed that there is a statistically significant difference ($p < 0.05$) between the mean observed TCE degradation over 24 h for the nZVI- and Fe^{2+}-activated persulfate systems.

The remaining MTBE concentration was ∼60% of the initial MTBE concentration using nZVI-activated persulfate compared to >80% using either granular ZVI or nZVI systems (Figure 1d). MTBE is more recalcitrant than the other organic compounds explored because of the binding of *tert*-butyl with ether.[28]

These findings clearly indicate that nZVI-activated persulfate is a promising system to treat hazardous organic compounds (e.g., TCE, MTBE, naphthalene, and chlorobenzene) compared to iron reduction methods (e.g., granular ZVI and nZVI). On the basis of these screening data, we choose to further investigate the behavior of the nZVI-activated persulfate system to treat TCE because the nZVI-activated persulfate system was more effective in treating TCE compared to the other hazardous organic compounds.

3.2. TCE Treatment. Degradation of TCE by the various persulfate systems explored (Figure 2) illustrates how the various systems behave. Over a 3-h reaction period, TCE treatments using Fe^{2+}-activated persulfate and granular-ZVI-activated persulfate were very similar. In comparison, Oh et al.[19] indicated that the oxidation of poly(vinyl alcohol) (PVA) with ZVI-activated persulfate (>99%) was higher than that of Fe^{2+}-activated persulfate (∼70%) over a 2-h reaction period for an activator to persulfate molar ratio of 1:1. Padmanabhan[29] reported the same observation with TCE; however, Padmanabhan[29] and Oh et al.[19] used microsized ZVI and not the

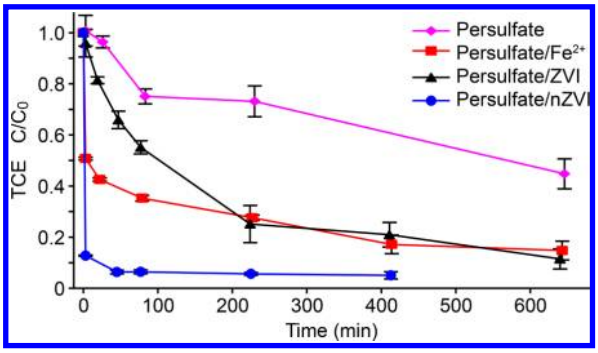

Figure 2. TCE treatment by unactivated persulfate (persulfate) and activated persulfate (persulfate/Fe^{2+} (ferrous iron activated), persulfate/ZVI (granular ZVI activated), and persulfate/nZVI (nZVI activated)). The error bars represent the standard deviation from three replicates.

dx.doi.org/10.1021/ie400387p | *Ind. Eng. Chem. Res.* 2013, 52, 13564−13571

granular size as used in this study. Thus, we hypothesize that the difference between these findings is due to the size of the ZVI materials used, where the larger surface area gives rise to an increased capability to activate persulfate (and other like oxidants).

The initial TCE degradation rate (defined over the initial 3 min) by nZVI-activated persulfate was 1.11×10^{-4} M min^{-1} compared to initial degradation rates of 6.25×10^{-5}, 5.18×10^{-6}, and 1.8×10^{-7} M min^{-1} for Fe^{2+}-activated persulfate, ZVI-activated persulfate, and unactivated persulfate, respectively. Although the initial TCE reaction rate by nZVI-activated persulfate was very fast, after 45 min the reaction rate drastically reduced.

The late time (>26 min) pseudo-first-order TCE degradation rate coefficients[30] for nZVI-activated persulfate, ZVI-activated persulfate, Fe^{2+}-activated persulfate, and unactivated persulfate were 1.1×10^{-5} ($r^2 = 0.98$), 4.3×10^{-5} ($r^2 = 0.93$), 2.7×10^{-5} ($r^2 = 0.94$), and 1.8×10^{-5} s^{-1} ($r^2 = 0.94$), respectively. The change from the initially fast TCE reaction rate to a very slow reaction rate for the nZVI-activated persulfate system is suspected to be caused by consumption of persulfate, depletion of nZVI particles, or passivation of reaction sites on the nZVI particles. We explore and discuss these potential causes below.

To advance our understanding of the role nZVI plays as an activator for persulfate, we conducted a separate series of experiments in the absence of TCE. As expected, the more nZVI in the system, the more persulfate was consumed (Figure 3a). At a persulfate/nZVI molar ratio of 1:5, >99% of the persulfate was consumed, while at a persulfate/nZVI molar ratio of 1:1 [as we used in the previous experiment to treat TCE], <30% of the persulfate was consumed over a 5-day reaction period. Thus, there was an excess of persulfate in the system at a persulfate/nZVI molar ratio of 1:1.

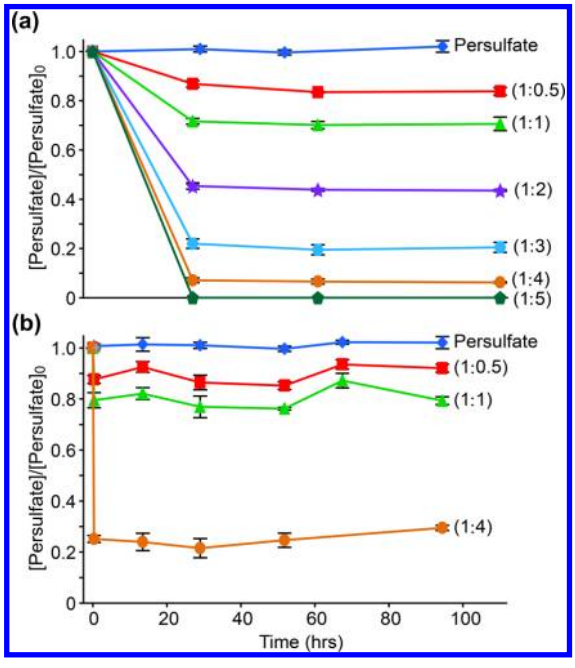

Figure 3. Persulfate decomposition for different persulfate to iron molar ratios for (a) the persulfate/nZVI system and (b) the persulfate/Fe^{2+} system. The persulfate-only system (control) is shown by the diamonds (◆), and the line legends for the remaining data indicate the molar ratio of persulfate to iron. The initial persulfate concentration was 1.8 g L^{-1} (9.4×10^{-3} M). The error bars represent the standard deviation from three replicates.

Similarly, when Fe^{2+} is used as an activator for persulfate at a persulfate/Fe^{2+} molar ratio of 1:1, only ~20% of persulfate is consumed (Figure 3b). However, the ability of the nZVI system to consume persulfate was higher than that of the Fe^{2+} system. For example, the persulfate residuals at a persulfate/Fe^{2+} and persulfate/nZVI system molar ratio of 1:4 were ~25% and 7%, respectively. Liang et al.[31] found that, at a TCE/persulfate/Fe^{2+} molar ratio of 1:20:20, 43% of persulfate and 36% of TCE remained in the system at the end of the reaction period. At the same molar ratio, we found that ~45% of TCE and ~80% of persulfate remained. The difference in these results may be related to the system pH. The initial pH in the study by Liang et al.[31] was 4.5, while the pH in our study was ~6.5. At a lower pH, Fe^{2+} is more soluble and available in the aqueous system;[17,18] however, both studies are in general agreement on the residual amount of persulfate and TCE in the system.

The form of the iron in the persulfate/nZVI system was investigated (Figure 4a). In the absence of persulfate, ≤8% of nZVI was transferred into the dissolved phase (Fe^{2+} and Fe^{3+}) because of the natural corrosion of nZVI in an aqueous system (eq 6). In the presence of persulfate, >30% of nZVI was transferred into the dissolved phase, and most of this was in the Fe^{3+} state because of the high corrosion of nZVI by persulfate (eq 5). As mentioned earlier, nZVI can activate persulfate indirectly by, initially, releasing Fe^{2+} into the aqueous systems, and then the released Fe^{2+} can activate persulfate directly to generate free radicals. The final iron state in this system is Fe^{3+}

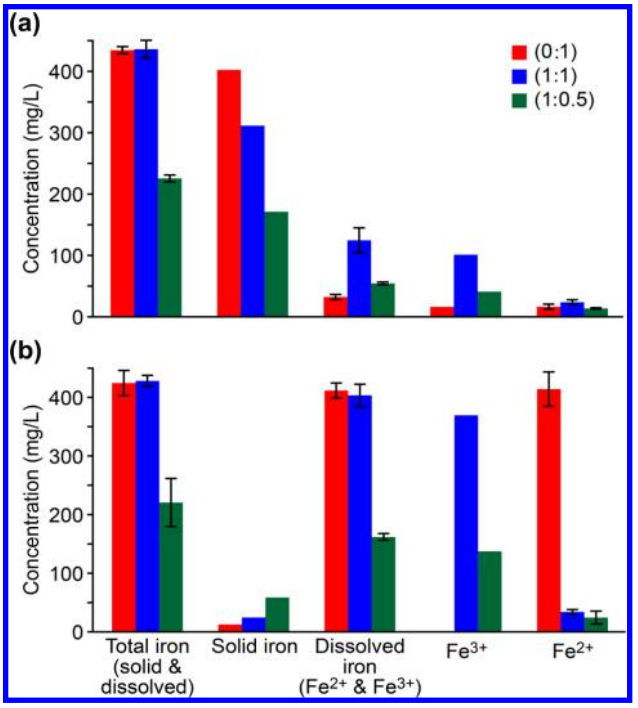

Figure 4. State of iron for different initial persulfate-to-iron molar ratios for (a) persulfate/nZVI system and (b) persulfate/Fe^{2+} system. The reaction period was 26 h for the persulfate/nZVI system and 50 min for the persulfate/Fe^{2+} system. The bar legend indicates the molar ratio of persulfate to iron. The initial persulfate concentration was 1.8 g L^{-1} (9.4×10^{-3} M), and no persulfate was present in the (0:1) system. The error bars represent the standard deviation from three replicates.

dx.doi.org/10.1021/ie400387p | Ind. Eng. Chem. Res. 2013, 52, 13564−13571

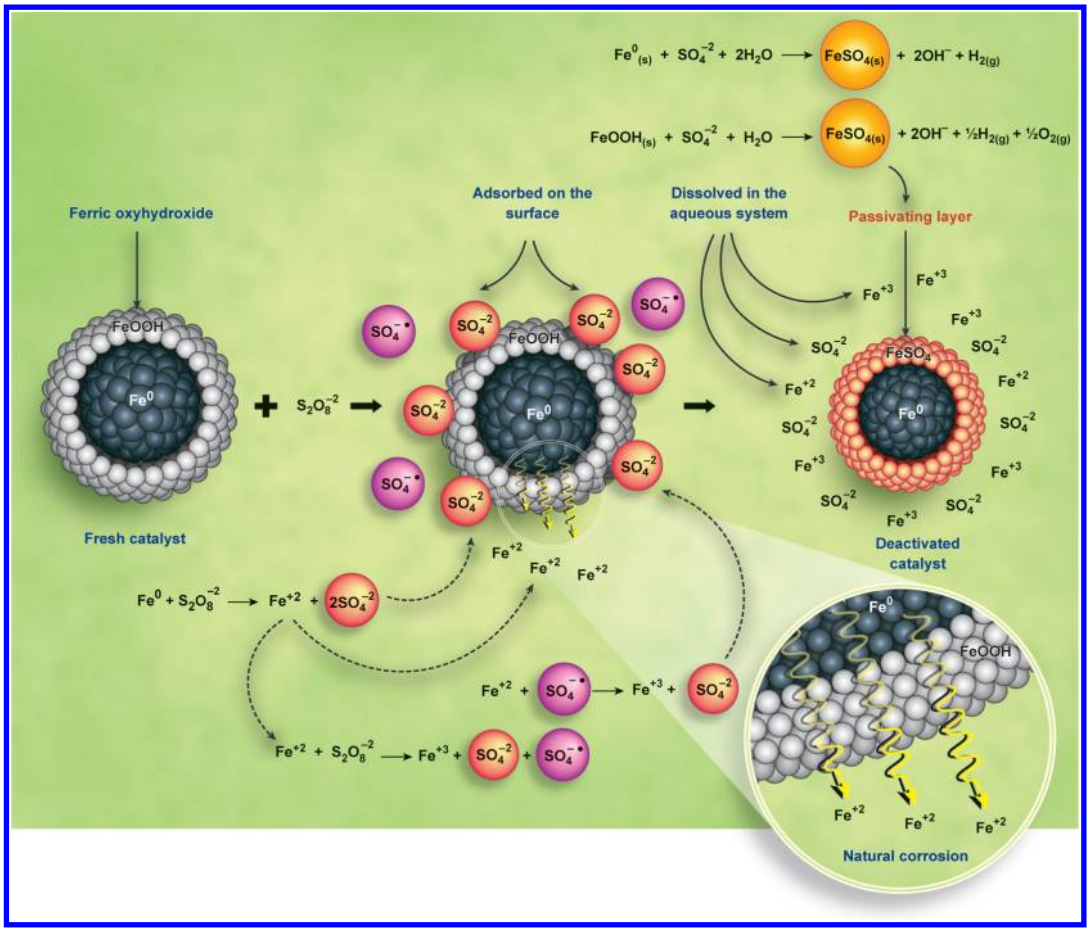

Figure 5. Conceptual model that illustrates the formation of an iron sulfate complex on the surface of a nZVI particle.

(eq 8). Theoretically, all nZVI should be converted into Fe^{3+} as an indicator of the complete depletion of nZVI. Experimentally, we found that only 23% of nZVI was converted into Fe^{3+}, but the amount of Fe^{3+} in the persulfate/nZVI system was almost 4 times higher than that in the system with only nZVI present. However, the remaining nZVI was not able to react with persulfate, suggesting that deactivation of the nZVI surfaces occurred.

In contrast to the persulfate/nZVI system, >85% of Fe^{2+} was converted into Fe^{3+} in the persulfate/Fe^{2+} system (Figure 4b). The remaining dissolved Fe^{2+} in the persulfate/Fe^{2+} system is not able to react with persulfate. In addition, we visually observed precipitates and quantified the suspended iron, which is likely a result of the following reaction pathway:

$$Fe^{3+} + 3H_2O \rightarrow Fe(OH)_3 \downarrow + 3H^+ \quad (11)$$

Moreover, the small amount of Fe^{2+} (~8%) that was left in the system (Figure 4b) is below the minimum threshold concentration, which allows the reaction to proceed.

3.3. Characterization of the nZVI Surface. *3.3.1. Fresh nZVI Surface.* The main form of iron on the active activator surface (not exposed to persulfate) was found to be FeOOH (ferric oxyhydroxide), which is consistent with that of Li et al.,[32] Li et al.,[33] and Sun et al.[34] Figure S1a (see the Supporting Information, SI) shows that the BE of the main peak in the iron spectra (Fe $2p_{3/2}$) was at 710.7 eV. Two main peaks were detected in the oxygen spectra (O 1s) at BEs of 529.4 and 530.7 eV (Figure S1b in the SI). The first main peak in the oxygen spectra (O 1s) implies the presence of the lattice oxygen (O^{2-}), while the second main peak is an indication of the presence of HO^- (hydroxyl group), as found by Haber et al.[35] FeO, Fe_3O_4, Fe_2O_3, or $Fe(OH)_3$ have only one main peak in their oxygen spectra (O 1s), but we observed two main peaks in the oxygen spectra, which supports the presence of FeOOH on the fresh nZVI particles. Furthermore, Li et al.,[33] Baltrusaitis et al.,[36] and Legrand et al.[37] found that FeOOH has a main peak in the iron spectra (Fe $2p_{3/2}$) at a BE of 710.8 (±0.2) eV, and two main peaks in the oxygen spectra (O 1s), one at 529.6 (±0.1) eV for O^{2-} and the second at 530.8 (±0.2) eV for HO^-. Our results are consistent with these observations. Thus, FeOOH is most likely formed on the surface of the fresh nZVI particles.

The mechanism responsible for forming FeOOH on the surface of nZVI particles starts by the release of Fe^{2+} into the aqueous system (eq 7), followed by the generation of Fe^{3+} under anaerobic conditions as given by

$$Fe^{2+} + H_2O \rightarrow Fe^{3+} + OH^- + \frac{1}{2}H_2 \quad (12)$$

Fe^{3+} is adsorbed on the surface of the nZVI particles, as suggested by Fu et al.,[38] and then continues to react and yield $Fe(OH)_3$ as an intermediate product to form FeOOH:[33]

$$Fe^{3+}(ads) + 3OH^- \rightarrow Fe(OH)_3(s) \quad (13)$$

$$Fe^{3+}(ads) + 3H_2O \rightarrow Fe(OH)_3(s) + 3H^+ \quad (14)$$

$$Fe(OH)_3(s) \rightarrow FeOOH(s) + H_2O \quad (15)$$

dx.doi.org/10.1021/ie400387p | Ind. Eng. Chem. Res. 2013, 52, 13564−13571

3.3.2. Deactivated nZVI Surface. The main form on iron of the deactivated nZVI surface (exposed to persulfate) was found to be iron sulfate. Figure S1d in the SI displays the iron spectra (Fe $2p_{3/2}$) of the deactivated nZVI surface, which was found at a BE of 711.1 eV. The main peak in the oxygen spectra (O 1s) was found at a BE of 531.5 eV, as shown in Figure S1e in the SI. Grosvenor et al.[39] and Frost et al.[40] detected $FeSO_4$ at a BE of 710.9 (±0.2) eV in the iron spectra (Fe $2p_{3/2}$) and at a BE of 532.0 eV in the oxygen spectra (O 1s). These findings are similar to those that we observed.

In addition, parts c and f of Figure S1 in the SI show the sulfur spectra (S 2p) of fresh and deactivated surfaces, respectively. Sulfur was not detectable on the fresh nZVI surface compared to a significant detectable sulfur peak on the deactivated nZVI surface at a BE of 168.6 eV, which implies the presence of sulfur as sulfate (e.g., $FeSO_4$, $Fe_2(SO_4)_3$) rather than sulfide (e.g., FeS, FeS_2) or other sulfur forms.[36,39−46] In the peer-reviewed literature,[42,44,46] the reference peaks of $FeSO_4$ in the sulfur spectra (S 2p) were detected at 169.0 (±0.2) eV. Therefore, ferrous sulfate ($FeSO_4$) is most likely formed on the deactivated nZVI surface.

The proposed mechanism to form ferrous sulfate ($FeSO_4$) on the deactivated nZVI surface from ZVI (directly) or from FeOOH (indirectly) is based on adsorbing sulfate anions (SO_4^{2-}) on the surfaces of the iron particles as follows:

$$Fe^0(s) + SO_4^{2-} + 2H_2O \rightarrow FeSO_4(s) + 2OH^- + H_2(g) \quad (16)$$

$$FeOOH(s) + SO_4^{2-} + H_2O \rightarrow FeSO_4(s) + 2OH^- + \frac{1}{2}H_2(g) + \frac{1}{2}O_2(g) \quad (17)$$

Parfitt and Smart[47,48] suggested that the sulfate anion (SO_4^{2-}) is adsorbed on the surface of iron oxides such as FeOOH by replacing two surface hydroxyl groups (OH^-) by one sulfate ion (SO_4^{2-}) to make a complex with binuclear bridging Fe−O—$S(O_2)$—O−Fe. In addition, a mononuclear bridging complex can be formed on the surface of iron oxides (i.e., FeOOH) like Fe−O—$S(O_2)$—O−H, as observed by Peak et al.[49]

Figure 5 provides a conceptual model that illustrates the sequence required to form the iron sulfate complex on the surface of a nZVI particle.

3.4. Optimal TCE Treatment Conditions. Generally, increasing the nZVI concentration enhanced TCE treatment until a persulfate/nZVI molar ratio of 1:1 was reached (Figure 6). Subsequently, further increases in nZVI resulted in no further improvement in TCE treatment, likely as a result of the various scavenging reaction pathways (eq 9).

TCE residuals (~7%) were similar between the TCE/persulfate/nZVI molar ratios of 1:20:20 and 1:40:20. The highest TCE treatment was at the molar ratios of 1:40:40 (96.3%) and 1:20:150 (96.1%). However, the optimum molar ratio was chosen to be at the TCE/persulfate/nZVI molar ratio of 1:20:20 (92.9%) based on the amount of materials (activator and oxidant) that was used to achieve this treatment level.

According to Oh et al.,[19] the treatment of PVA was maximized when the molar ratio between persulfate and Fe^{2+} (and also with persulfate to granular ZVI) was 1:1. Likewise, Liang et al.[31] found that the highest TCE treatment was at a TCE/persulfate/Fe^{2+} molar ratio of 1:20:15 and increased Fe^{2+} concentrations caused a decrease in TCE treatment. Thus, their observations are consistent with the results that we present here.

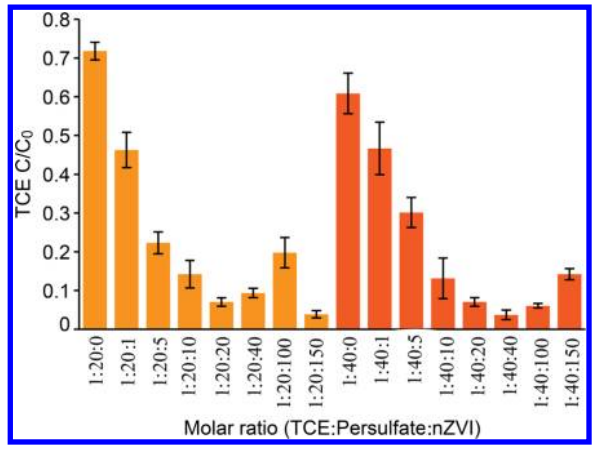

Figure 6. TCE treatment for the various TCE/persulfate/nZVI molar ratios explored. The reaction period was 16 h. The initial TCE concentration was 1.8 g L^{-1} (9.4×10^{-3} M). The error bars represent the standard deviation from five replicates.

The pH and redox potential of the persulfate/nZVI system were also investigated (Figure 7). As the amount of nZVI is increased in this system, the pH decreases from 4.5 for a persulfate-only system to just above 2 for a persulfate/nZVI molar ratio of 1:1 because of production of HSO_4^- from persulfate decomposition as given by[50]

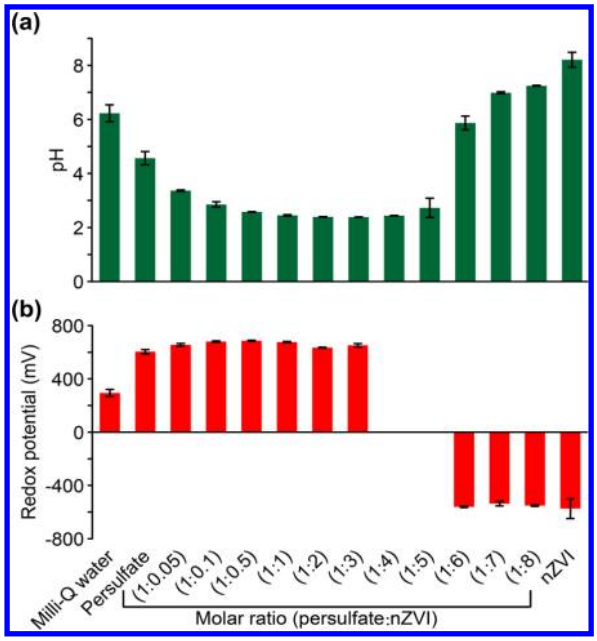

Figure 7. (a) System pH and (b) redox potential for a range of a persulfate-to-nZVI molar ratios explored, as indicated by the ratio in parentheses. Also shown are the pH and redox potential data for Milli-Q water only, persulfate solution only, and an nZVI-only system. The initial persulfate concentration was 1.8 g L^{-1} (9.4×10^{-3} M). The error bars represent a standard deviation from three replicates.

$$S_2O_8^{2-} + OH^- \rightarrow HSO_4^- + SO_4^{2-} + \frac{1}{2}O_2 \quad (18)$$

and then increases to near 7 for a persulfate/nZVI molar ratio of 1:8. At a persulfate/nZVI molar ratio of 1:5, insignificant

persulfate mass remains (Figure 3a) and the pH is controlled by the production of hydroxyl anions (OH^-; eqs 6 and 7) and the passivation state of the nZVI particles present. Once all of the persulfate is consumed in the vicinity of a persulfate/nZVI molar ratio of 1:5, the system transitions from oxidizing to reducing conditions.

Despite a general decrease in the TCE treatment effectiveness above a persulfate/nZVI molar ratio of 1:1, there was an apparent anomaly for a TCE/persulfate/nZVI molar ratio of 1:20:150 (Figure 6). We speculate that this anomaly was a result of the initial degradation of TCE due to oxidation reactions until all of the persulfate was depleted and then the system became reducing, and further degradation of TCE was a result of the reaction between nZVI and TCE following the reductive dechlorination pathway given by

$$3Fe^0 + C_2HCl_3 + 3H^+ \rightarrow 3Fe^{2+} + C_2H_4 + 3Cl^- \quad (19)$$

This reaction pathway is supported by the pH and redox observations of the nZVI/persulfate system (Figure 7).

4. SUMMARY

In this study, a method was applied to treat selective hazardous organic compounds (i.e., TCE, MTBE, naphthalene, and chlorobenzene) using nZVI particles and persulfate. The results show that coupling nZVI or granular ZVI with persulfate is more effective to treat the selective organic compounds than using either nZVI or granular ZVI alone.

The focused investigation of the degradation of TCE by the nZVI-activated persulfate system indicated that the degradation rate was initially very fast but then reduced in <50 min to a magnitude representative of an unactivated persulfate system. The suggested scenario is that the nZVI surfaces were deactivated or passivated as a result of the reaction with persulfate. To support this hypothesis, the persulfate/nZVI system without TCE present was explored. After ~5 days of exposure to persulfate, the reaction with nZVI essentially stopped with <25% of the nZVI mass converted into dissolved Fe^{3+} and >70% of the initial persulfate remaining. The results from XPS analyses showed that iron sulfate (i.e., ferrous sulfate $FeSO_4$) was present on the nZVI surface following exposure to persulfate compared to iron oxide−hydroxide (i.e., FeOOH) on the fresh nZVI surface.

■ ASSOCIATED CONTENT

Supporting Information

Analyses of nZVI surfaces by XPS. This material is available free of charge via the Internet at http://pubs.acs.org.

■ AUTHOR INFORMATION

Corresponding Author

*Tel.: 1 519 888 4567 ext. 32111. Fax: 1 519 888 4349. E-mail: nthomson@uwaterloo.ca.

Notes

The authors declare no competing financial interest.

■ ACKNOWLEDGMENTS

Financial support for this investigation was provided by a King Abdul-Aziz City for Science & Technology (KACST) Scholarship (to M.A.A.) and a Natural Sciences and Engineering Research Council (NSERC) of Canada Collaborative Research and Development Grant (to N.R.T.).

■ REFERENCES

(1) Kester, J. E.; Clewell, H. J. The perils and promise of modern risk assessment: the example of trichloroethylene. *Clin. Occup. Environ. Med.* **2004**, *4* (3), 497−512.

(2) Wernke, M.; Schell, J. Solvents and malignancy. *Clin. Occup. Environ. Med.* **2004**, *4* (3), 513−527.

(3) NTP. *Report on carcinogens background document for Methyl Tertiary-Butyl Ether*; National Toxicology program; U.S. Department of Health and Human Services: Washington, DC, 1998.

(4) NTP. *Report on carcinogens background document for Napthalene*; National Toxicology Program; U.S. Department of Health and Human Services: Washington, DC, 2002.

(5) NTP. *Report on carcinogens background document for Chlorobenzene*; National Toxicology Program; U.S. Department of Health and Human Services: Washington, DC, 1985.

(6) Tsai, T. T.; Kao, C. M.; Yeh, T. Y.; Lee, M. S. Chemical oxidation of chlorinated solvents in contaminated groundwater: Review. *Pract. Period. Hazard., Toxic, Radioact. Waste Manage.* **2008**, *12* (2), 116−126.

(7) Xu, X.; Thomson, N. R. Hydrogen Peroxide Persistence in the Presence of Aquifer Materials. *Soil Sediment Contam.* **2010**, *19* (5), 602−616.

(8) Xu, X.; Thomson, N. R. A long-term bench-scale investigation of permanganate consumption by aquifer materials. *J. Contam. Hydrol.* **2009**, *110* (3−4), 73−86.

(9) Russo, L.; Rizzo, L.; Belgiorno, V. PAHs contaminated soils remediation by ozone oxidation. *Desalin. Water Treat.* **2010**, *23* (1−3), 161−172.

(10) Sra, K. S.; Thomson, N. R.; Barker, J. F. Persistence of Persulfate in Uncontaminated Aquifer Materials. *Environ. Sci. Technol.* **2010**, *44* (8), 3098−3104.

(11) Killian, P. F.; Bruell, C. J.; Liang, C.; Marley, M. C. Iron(II) Activated Persulfate Oxidation of MGP Contaminated Soil. *Soil Sediment Contam.* **2007**, *16* (6), 523−537.

(12) Liang, C.; Liang, C. P.; Chen, C. C. pH dependence of persulfate activation by EDTA/Fe(III) for degradation of trichloroethylene. *J. Contam. Hydrol.* **2009**, *106* (3−4), 173−182.

(13) Liang, C.; Wang, Z. S.; Bruell, C. J. Influence of pH on persulfate oxidation of TCE at ambient temperatures. *Chemosphere* **2007**, *66* (1), 106−113.

(14) Norman, R. O. C.; Storey, P. M.; West, P. R. Electron spin resonance studies. Part XXV. Reactions of the sulphate radical anion with organic compounds. *J. Chem. Soc. B* **1970**, 1087−1095.

(15) Anbar, M.; Neta, P. A compilation of specific bimolecular rate constants for the reactions of hydrated electrons, hydrogen atoms and hydroxyl radicals with inorganic and organic compounds in aqueous solution. *Int. J. Appl. Radiat. Isot.* **1967**, *18* (7), 493−523.

(16) House, D. A. Kinetics and mechanism of oxidations by peroxydisulfate. *Chem. Rev.* **1962**, *62*, 185−203.

(17) Pignatello, J. J.; Baehr, K. Ferric complexes as catalysts for Fenton degradation of 2,4-D and metolachlor in soil. *J. Environ. Qual.* **1994**, *23* (2), 365−370.

(18) Sun, Y.; Pignatello, J. J. Chemical treatment of pesticide wastes. Evaluation of iron(III) chelates for catalytic hydrogen peroxide oxidation of 2,4-D at circumneutral pH. *J. Agric. Food Chem.* **1992**, *40* (2), 322−327.

(19) Oh, S. Y.; Kim, H. W.; Park, J. M.; Park, H. S.; Yoon, C. Oxidation of polyvinyl alcohol by persulfate activated with heat, Fe^{2+}, and zero-valent iron. *J. Hazard. Mater.* **2009**, *168* (1), 346−351.

(20) Liang, C.; Lai, M. C. Trichloroethylene degradation by zero valent iron activated persulfate oxidation. *Environ. Eng. Sci.* **2008**, *25* (7), 1071−1077.

(21) Oh, S.-Y.; Kang, S.-G.; Chiu, P. C. Degradation of 2,4-dinitrotoluene by persulfate activated with zero-valent iron. *Sci. Total Environ.* **2010**, *408* (16), 3464−3468.

(22) Liang, C.; Guo, Y. Y. Mass Transfer and Chemical Oxidation of Naphthalene Particles with Zerovalent Iron Activated Persulfate. *Environ. Sci. Technol.* **2010**, *44* (21), 8203−8208.

(23) Furukawa, Y.; Kim, J. W.; Watkins, J.; Wilkin, R. T. Formation of ferrihydrite and associated iron corrosion products in permeable reactive barriers of zero-valent iron. *Environ. Sci. Technol.* **2002**, *36* (24), 5469−5475.
(24) Liang, C.; Su, H.-W. Identification of Sulfate and Hydroxyl Radicals in Thermally Activated Persulfate. *Ind. Eng. Chem. Res.* **2009**, *48* (11), 5558−5562.
(25) *Standard Practice for Fast Screening for Volatile Organic Compounds in Water Using Solid Phase Microextraction (SPME)*; ASTM: West Conshohocken, PA, 2003; ASTM-D6889-03.
(26) Liang, C.; Huang, C.-F.; Mohanty, N.; Kurakalva, R. M. A rapid spectrophotometric determination of persulfate anion in ISCO. *Chemosphere* **2008**, *73* (9), 1540−1543.
(27) *Standard methods for the examination of water and wastewater*, 17th ed.; APHA: Washington, DC, 1989.
(28) Chen, K. F.; Kao, C. M.; Wu, L. C.; Surampalli, R. Y.; Liang, S. H. Methyl Tert-Butyl Ether (MTBE) Degradation by Ferrous Ion-Activated Persulfate Oxidation: Feasibility and Kinetics Studies. *Water Environ. Res.* **2009**, *81*, 687−694.
(29) Padmanabhan, A. R. *Novel Simultaneous Reduction/Oxidation Process for Destroying Organic Solvents*; Worcester Polytechnic Institute: Worcester, MA, 2008.
(30) Levenspiel, O. *Chemical Reaction Engineering*, 3rd ed.; John Wiley & Sons: New York, 1999.
(31) Liang, C.; Bruell, C. J.; Marley, M. C.; Sperry, K. L. Persulfate oxidation for in situ remediation of TCE. I. Activated by ferrous ion with and without a persulfate−thiosulfate redox couple. *Chemosphere* **2004**, *55* (9), 1213−1223.
(32) Li, L.; Fan, M.; Brown, R. C.; Van Leeuwen, J.; Wang, J.; Wang, W.; Song, Y.; Zhang, P. Synthesis, properties, and environmental applications of nanoscale iron-based materials: A review. *Crit. Rev. Environ. Sci. Technol.* **2006**, *36* (5), 405−431.
(33) Li, X. Q.; Cao, J.; Zhang, W. X. Stoichiometry of Cr(VI) immobilization using nanoscale zero valent iron (nZVI): A study with high-resolution X-ray photoelectron spectroscopy (HR-XPS). *Ind. Eng. Chem. Res.* **2008**, *47* (7), 2131−2139.
(34) Sun, Y. P.; Li, X. Q.; Cao, J.; Zhang, W. X.; Wang, H. P. Characterization of zero-valent iron nanoparticles. *Adv. Colloid Interface Sci.* **2006**, *120* (1−3), 47−56.
(35) Haber, J.; Stoch, J.; Ungier, L. X-ray photoelectron spectra of oxygen in oxides of Co, Ni, Fe and Zn. *J. Electron Spectrosc. Relat. Phenom.* **1976**, *9* (5), 459−467.
(36) Baltrusaitis, J.; Cwiertny, D. M.; Grassian, V. H. Adsorption of sulfur dioxide on hematite and goethite particle surfaces. *Phys. Chem. Chem. Phys.* **2007**, *9* (41), 5542−5554.
(37) Legrand, D. L.; Bancroft, G. M.; Nesbitt, H. W. Oxidation/alteration of pentlandite and pyrrhotite surfaces at pH 9.3: Part 1. Assignment of XPS spectra and chemical trends. *Am. Mineral.* **2005**, *90* (7), 1042−1054.
(38) Fu, H.; Wang, X.; Wu, H.; Yin, Y.; Chen, J. Heterogeneous uptake and oxidation of SO_2 on iron oxides. *J. Phys. Chem. C* **2007**, *111* (16), 6077−6085.
(39) Grosvenor, A. P.; Kobe, B. A.; Biesinger, M. C.; McIntyre, N. S. Investigation of multiplet splitting of Fe 2p XPS spectra and bonding in iron compounds. *Surf. Interface Anal.* **2004**, *36*, 1564−1574.
(40) Frost, D. C.; Leeder, W. R.; Tapping, R. L. X-ray photoelectron spectroscopic investigation of coal. *Fuel* **1974**, *53* (3), 206−211.
(41) Nesbitt, H. W.; Muir, I. J. X-ray photoelectron spectroscopic study of a pristine pyrite surface reacted with water vapour and air. *Geochim. Cosmochim. Acta* **1994**, *58* (21), 4667−4679.
(42) Kelemen, S. R.; George, G. N.; Gorbaty, M. L. Direct determination and quantification of sulphur forms in heavy petroleum and coals. 1. The X-ray photoelectron spectroscopy (XPS) approach. *Fuel* **1990**, *69* (8), 939−944.
(43) Descostes, M.; Mercier, F.; Beaucaire, C.; Zuddas, P.; Trocellier, P. Nature and distribution of chemical species on oxidized pyrite surface: Complementarity of XPS and nuclear microprobe analysis. *Nucl. Instrum. Methods Phys. Res., Sect. B* **2001**, *181* (1−4), 603−609.
(44) Bukhtiyarova, G. A.; Bukhtiyarov, V. I.; Sakaeva, N. S.; Kaichev, V. V.; Zolotovskii, B. P. XPS study of the silica-supported Fe-containing catalysts for deep or partial H_2S oxidation. *J. Mol. Catal. A: Chem.* **2000**, *158* (1), 251−255.
(45) Baltrus, J. P.; Diehl, J. R. Surface spectroscopic studies of factors influencing xanthate adsorption on coal pyrite surfaces. *Surf. Interface Anal.* **1997**, *25* (2), 64−70.
(46) Descostes, M.; Mercier, F.; Thromat, N.; Beaucaire, C.; Gautier-Soyer, M. Use of XPS in the determination of chemical environment and oxidation state of iron and sulfur samples: constitution of a data basis in binding energies for Fe and S reference compounds and applications to the evidence of surface species of an oxidized pyrite in a carbonate medium. *Appl. Surf. Sci.* **2000**, *165* (4), 288−302.
(47) Parfitt, R. L.; Smart, R. S. C. The mechanism of sulfate adsorption on iron oxides. *Soil Sci. Soc. Am. J.* **1978**, *42*, 48−50.
(48) Parfitt, R. L.; Smart, R. S. C. Infrared spectra from binuclear bridging complexes of sulphate adsorbed on goethite (α-FeOOH). *J. Chem. Soc., Faraday Trans. 1* **1977**, *73*, 796−802.
(49) Peak, D.; Ford, R. G.; Sparks, D. L. An in situ ATR-FTIR investigation of sulfate bonding mechanisms on goethite. *J. Colloid Interface Sci.* **1999**, *218* (1), 289−299.
(50) Siegal, J.; Rees, A. A.; Eggers, K. W.; Hobbs, R. L. In situ chemical oxidation of residual LNAPL and dissolved-phase fuel hydrocarbons and chlorinated alkenes in groundwater using activated persulfate. *Remediation* **2009**, *19* (2), 19−35.